

Mechanisms and kinetics of Al-Si ordering in anorthite: I. Incommensurate structure and domain coarsening

MICHAEL A. CARPENTER

Department of Earth Sciences, University of Cambridge, Downing Street, Cambridge CB2 3EQ, England

ABSTRACT

The first crystals to form on heating anorthite glass at temperatures of ~1100–1400 °C have substantial Al-Si disorder. This metastable disorder is reduced by prolonged annealing, and the ordering process has been followed by transmission electron microscopy. Ordering initially gives rise to an incommensurate superstructure with diffuse type e reflections in electron diffraction patterns. As a function of annealing time the e reflections change orientation and become sharper and closer together. The measured spacings and orientations of the incommensurate repeat are remarkably similar to those shown by crystals of the ordered intermediate plagioclase feldspar solid solution and depend primarily on the degree of order attained rather than on composition. At longer annealing times, the incommensurate structure gives way to the stable $I\bar{1}$ ordered state in an apparently continuous manner; the activation energy for this transition was found to be 135 ± 14 kcal/mol. Type b APDs then coarsen according to the expected rate law

$$\delta^n - \delta_0^n = nk e^{(-\Delta H^*/RT)}(t - t_0)$$

where n is constrained to have values between ~2 and ~2.6, k is between 0.44×10^{-4} Å²/h (for $n = 2$) and 32.6 Å^{2.6}/h (for $n = 2.6$), and ΔH^* is between 121 and 152 kcal/mol. A qualitative picture of the incommensurate structure as arising from the interaction of two component ordering schemes with $C\bar{1}$ and $I\bar{1}$ symmetry is outlined. The order parameters for these two component structures could have strong interactions via their associated elastic strains.

INTRODUCTION

This study of the mechanisms and kinetics of Al-Si ordering in anorthite was prompted by the need to characterize the phase transitions that occur in the end-member phases of the plagioclase feldspar solid solution before turning to the more complex subsolidus behavior of crystals with intermediate compositions. A great deal is known about ordering in albite, but quantitative aspects of the ordering behavior of anorthite seem to have been relatively neglected. A new approach has also been stimulated by recent advances in the theoretical analysis of structural phase transitions in minerals based on Landau theory (see reviews by Salje 1988a, 1988b, 1989; Carpenter, 1988, 1991a; Carpenter and Salje, 1989). The aims of the study were, first, to investigate the manner in which anorthite crystals evolve under nonequilibrium conditions; second, to test predicted rate laws for ordering and antiphase domain coarsening; and finally to relate structural changes and the observed kinetic effects to the underlying thermodynamic driving forces. The results of transmission electron microscope (TEM) observations are reported in this paper. Calorimetric and spontaneous strain data are given in an accompanying paper (Carpenter, 1991b), along with a kinetic model based on the Ginzburg-Landau rate equation.

The literature on feldspars is vast. Readers are referred to recent reviews by Brown (1984), Smith and Brown (1988), and Carpenter (1988) for background and bibliographic information. It is sufficient to reiterate here that, under equilibrium conditions, anorthite crystals have $I\bar{1}$ symmetry above ~240 °C and retain a high degree of long range Al-Si order until they melt at ~1557 °C. In the absence of melting, there would be an equilibrium order-disorder transition ($C\bar{1} \rightleftharpoons I\bar{1}$) near 2000 °C. The equilibrium degree of order varies somewhat with temperature (see Benna et al., 1985; Carpenter et al., 1990; and references therein), but a much greater range of structural states can be obtained by heating anorthite glass at temperatures of ~1000–1500 °C. Under these conditions, the first crystals to form have a high degree of metastable disorder and essentially $C\bar{1}$ symmetry. On further annealing, the crystals evolve toward more ordered $I\bar{1}$ states. The results of Goldsmith and Laves (1956), Kroll and Müller (1980), and John and Müller (1988) concerning the ordering process in synthetic anorthite crystals prepared in this way have been used as the starting point for the present work. As described below, the ordering involves an incommensurate (IC) superstructure that appears to be remarkably similar to the intermediate plagioclase structure found in slowly cooled natural crystals

with compositions between $\sim\text{An}_{25}$ and $\sim\text{An}_{75}$. A preliminary report of this IC structure has been given by Carpenter and Salje (1989).

EXPERIMENTAL METHODS

All the observations presented in this paper and the accompanying paper (Carpenter, 1991b) were made on anorthite crystals synthesized from 250 g of glass. This glass was produced at the National Physical Laboratory by melting reagent grade SiO_2 and Al_2O_3 with natural calcite at $\sim 1680^\circ\text{C}$ in a Pt bucket for ~ 3 h. The melt was stirred at an intermediate stage before being poured into a steel mold and then allowed to cool in air. The resulting block of clear glass was finally annealed at $\sim 800^\circ\text{C}$ for ~ 30 min to relieve internal stresses. Electron microprobe analysis of a section of the glass showed that, within normal experimental uncertainty limits, the composition was stoichiometric $\text{CaAl}_2\text{Si}_2\text{O}_8$.

Crystallization of the glass was carried out at temperatures of 1100, 1200, 1300, and 1400°C . Approximately 0.4, 0.45, or 0.5 g batches of glass, sawn into cubes with edge dimensions of ~ 2 mm, were wrapped in Pt foil envelopes, placed in Pt buckets, and lowered into standard vertical resistance furnaces. Temperature was monitored throughout each annealing experiment with a Pt/Pt, 13% Rh thermocouple placed within a few millimeters of the sample, and uncertainty is considered to have been $\pm 3^\circ\text{C}$. Typically, several minutes elapsed before a sample reached the desired annealing temperature after it had been lowered into a hot furnace. The time scale for experiments of less than ~ 15 min is therefore somewhat arbitrary, and these experiments were deemed to have started when the temperature close to the sample was within $\sim 25^\circ\text{C}$ of the desired annealing temperature, usually 1.25 or 1.5 min after loading. The same procedure was followed for every heat treatment, so that all the crystalline anorthite produced at a given temperature should have experienced similar crystallization conditions. Quenching was achieved simply by raising the bucket rapidly out of the furnace and allowing it to cool in air. The product from each experiment consisted of an aggregate of white cubes that were slightly sintered together; the edges and corners of the cubes also became rounded during the annealing period. Complete details of times and temperatures for each sample are given in Table 1 of Carpenter (1991b).

A single cube was selected from each product, set in epoxy resin, and mounted as a normal thin section. Optical examination showed that the cubes typically had a rim of crystals radiating in from the edges and a core of crystals with random orientations (Fig. 1). The crystals tended to show nonuniform extinction, though in products from the higher temperature annealing experiments, small crystals with more regular extinction could be distinguished on a scale of $\sim 40\ \mu\text{m}$ (Fig. 1). The core and rim textures presumably represent two types of nucleation of anorthite from the glass at the cube surfaces and randomly in the central portion. Relict glass was ob-

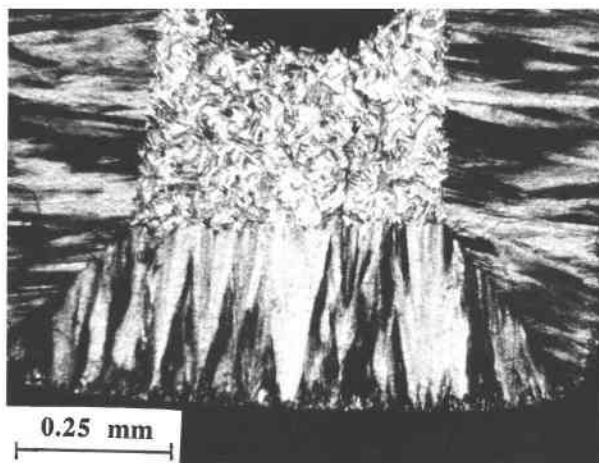


Fig. 1. Optical micrograph showing part of a thin section of one of the cubes of anorthite with a distinct core and rim texture. In the rim, individual crystallites are oriented with their long axes perpendicular to the surface, whereas in the core they appear to have random orientations. (Sample no. ANC74, 0.25 h, 1400°C .)

served optically only in crushed fragments from the products of the two shortest annealing experiments at 1100°C (ANC 19, 15 min; ANC 66, 20 min). Klein and Uhlmann (1974) have described the kinetics of crystallization of anorthite from glass under comparable conditions in more detail.

A Cu disc or Ti grid was glued to each cube that had been prepared as a thin section. The disc and sample were removed from the thin section and thinned with high energy Ar ions. The thinned crystals were then examined in an AEI EM6G electron microscope operated at 100 kV. Bright field images revealed the presence of abundant grain boundaries and subgrain boundaries, isolated dislocations, and pervasive submicroscopic lamellar twinning. As already reported by Kroll and Müller (1980) and John and Müller (1988), the twinning follows the albite twin law with $\{010\}$ as the twin plane. The scale of twinning varied to some extent as a function of annealing temperature, but there was also considerable variation within each sample. Crystals prepared at 1100°C tended to have a preponderance of the finest twins, whereas coarser twins tended to predominate in crystals synthesized at 1400°C (illustrated in Figs. 2a and 2b). In every sample examined, however, individual twins that were wider than $\sim 0.25\ \mu\text{m}$ were found and could be used to obtain selected area diffraction patterns. The twinning textures did not appear to change significantly with annealing time at a given temperature.

Approximately ten diffraction patterns were recorded from each sample. These were generally exposed on the photographic plate for longer than normal to facilitate the detection of weak and diffuse superlattice reflections. The sublattice reflections at $h + k = \text{even}$, $l = \text{even}$ positions were typically strong and sharp except where the fine-

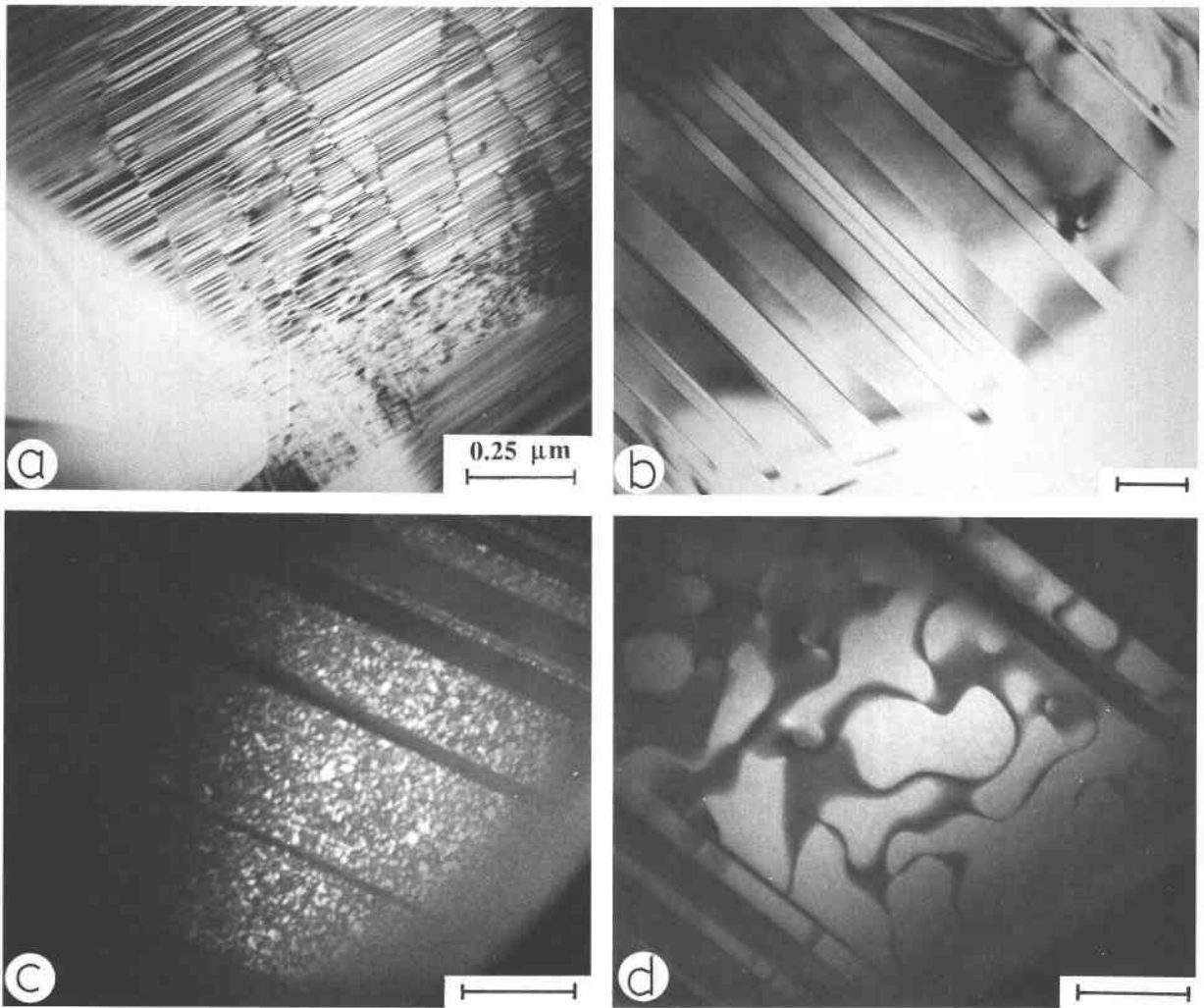


Fig. 2. Electron optical images of anorthite crystals synthesized from glass. (a) Finest scale of twinning observed (ANC66, 20 min, 1100 °C). (b) Coarser twins in sample no. ANC10 (1 min, 1400 °C). (c) Dark field image using a b reflection, showing fine scale APDs (ANC38, 1.5 h, 1400 °C). (d) As c showing coarser APDs (ANC35, 408 h, 1400 °C). Note that in c and d the twins do not appear to influence the APD distribution. (Scale bar = 0.25 μm in each micrograph.)

scale twinning gave rise to streaking along b^* . Many diffraction patterns with nonstandard orientations showed the presence of more or less diffuse pairs of e reflections about the $h + k = \text{odd}, l = \text{odd}$ positions. The orientation and length of a vector $2s$ describing the separation of these reflections was measured wherever possible. Diffraction patterns from crystals annealed for relatively long times contained sharp or diffuse b reflections instead of e reflections. Diffuse c reflections ($h + k = \text{even}, l = \text{odd}$) were present in all the diffraction patterns with appropriate orientations, and d reflections ($h + k = \text{odd}, l = \text{even}$) were observed in some diffraction patterns from the most ordered crystals.

When b reflections were observed, they were used to obtain dark field images of the associated antiphase domain (APD) textures. As illustrated by Kroll and Müller

(1980) and in Figures 2c and 2d, these b APDs have an equidimensional appearance and show no obvious interactions with twin boundaries. Only at grain boundaries has evidence of heterogeneous nucleation or coarsening of the APDs been observed (e.g., see Fig. 10a of Kroll and Müller, 1980). An average APD size was measured from each micrograph as the average spacing between antiphase boundaries (APBs) along straight lines placed randomly across the micrograph. Average values from approximately five micrographs were then used to calculate a mean value and its standard deviation for the sample (Table 1). Dark field images using pairs of e reflections were not obtained, largely because these reflections were weak and diffuse in comparison with the b reflections.

Also present in every sample examined by TEM were

small inclusions located at grain boundaries. They represented less than 1% of the sample and varied in size between a few hundred ångströms in the shorter, low temperature experiments and a few thousand ångströms in the longer, high temperature experiments. Weak and diffuse lines close to ~ 23.94 and $\sim 24.12^\circ 2\theta$, corresponding to spacings of ~ 3.72 and ~ 3.69 Å, were also observed in X-ray powder photographs from most of the synthetic samples. These could not be indexed either on the basis of triclinic anorthite or the orthorhombic and hexagonal polymorphs described by Davis and Tuttle (1952), Takéuchi and Donnay (1959), and Takéuchi et al. (1973). Similar powder lines from an unknown phase in the system $\text{MgO-Al}_2\text{O}_3\text{-SiO}_2$ were tentatively interpreted by Schreyer and Schairer (1962) as arising from a petalite-type structure. Electron diffraction patterns from the inclusions gave characteristic repeat lengths of ~ 7.8 and ~ 8.0 Å, however, which do not appear to be compatible with the lattice parameters of petalite itself, as given by Effenberger (1980). The extra powder lines may result from some other phase not identified by TEM, of course, and the inclusions remain unidentified. Their presence is probably owed to small concentrations of MgO derived from the natural calcite used as a starting material for preparing the glass. The apparent grain size of the inclusions coarsened with annealing temperature, and their number markedly decreased, suggesting that their total volume remained fixed. They are not thought to have influenced any of the experimental results presented in this paper or in the accompanying paper (Carpenter, 1991b).

No X-ray or electron-optical evidence was found for the presence of the hexagonal or orthorhombic polymorphs of $\text{CaAl}_2\text{Si}_2\text{O}_8$ in any of the experimental products.

INCOMMENSURATE ORDERING

Pairs of e reflections were observed most clearly in diffraction patterns containing \mathbf{b}^* and $[10\bar{l}]^*$ where l is 3, 4, 5, 6, or 7. The orientation of the vector $2\mathbf{s}$ between them was therefore measured in these sections of the reciprocal lattice as the angle between \mathbf{b}^* and \mathbf{s} . Some diffraction patterns with different zone axes, but still containing both members of each pair, then allowed the orientation of \mathbf{s} to be measured uniquely in three dimensions. The real space dimension of the IC structure, $|2\mathbf{s}|^{-1}$, was obtained by measuring the distance between a pair of e reflections in the diffraction patterns and applying a known camera constant. (Note that $|2\mathbf{s}|^{-1}$ gives the spacing between the periodic antiphase boundaries and that the wavelength of the IC repeat is actually $2/|2\mathbf{s}|$.)

The e reflections observed in diffraction patterns from anorthite crystals synthesized in the shortest experiment at 1100 °C (15 min) are exceedingly weak and diffuse. With longer annealing, they become stronger and sharper, and their orientations and spacings change systematically. An illustrative sequence is shown in Figure 3, and the complete data are given in Table 1 of Carpenter (1991b).

TABLE 1. Observed domain diameters, δ , for type b APDs in synthetic anorthite crystals prepared from glass

Sample no.	Annealing time (h)	Annealing temperature (°C)	δ (Å)
ANC38	1.5	1400	203 ± 32
ANC39	8.25	1400	324 ± 42
ANC36	48	1400	611 ± 116
ANC9	179	1400	1024 ± 130
ANC35	408	1400	1540 ± 141
ANC48	1102	1400	2283 ± 290
ANC43	48	1300	189 ± 21
ANC4	113	1300	223 ± 32
ANC45	400	1300	468 ± 59
ANC59	1077	1300	673 ± 120
ANC28	400	1200	140 ± 14
ANC31	1063	1200	169 ± 24

The orientation of \mathbf{s} rotates from approximately within the $\mathbf{b}^*\text{-}[10\bar{3}]^*$ plane to approximately within the $\mathbf{b}^*\text{-}[10\bar{6}]^*$ plane but remains within the range of orientations shown by \mathbf{s} in natural intermediate plagioclase crystals (Fig. 4). The range of $|2\mathbf{s}|^{-1}$ in the synthetic anorthite crystals, $\sim 25\text{--}90$ Å, also matches the range of values found for natural plagioclase crystals, though the largest value reported for a natural sample is 85 Å (McLaren, 1974). The sequence of structural states with increasing annealing time in the synthetic crystals mimics the effect of changing composition toward anorthite in the natural solid solution. In the last stages of this sequence, the e reflections are replaced by b reflections that are initially slightly elongate or diffuse but then become sharp (Fig. 3).

Comparison of the relationship between $\mathbf{b}^* \wedge \mathbf{s}$ and $|2\mathbf{s}|^{-1}$ shows that the diffraction characteristics of the natural and synthetic crystals are not identical, however (Fig. 5). For orientations and spacings corresponding to crystals with compositions $\sim \text{An}_{35}\text{--}\sim \text{An}_{55}$, the two sets of data are indistinguishable. They diverge at values of $|2\mathbf{s}|^{-1} > 40$ Å when \mathbf{s} for the synthetic anorthite crystals shows no further rotation with increasing $|2\mathbf{s}|^{-1}$. The e reflections from synthetic anorthite crystals also tend to be weaker and more diffuse than those from their natural counterparts, and no f reflections (pairs of reflections about the sublattice reflections) have yet been observed in anorthite.

Type c and d reflections arising from the $I\bar{1} \rightleftharpoons P\bar{1}$ transition show some variation with heat treatment. Crystals which give the weakest and most diffuse e reflections also give the weakest and most diffuse c reflections. The latter are elongate in the characteristic manner for anorthite crystals quenched from high temperatures (see Smith and Brown, 1988). Type d reflections were not observed in these diffraction patterns. As the e reflections become sharper, so also do the c reflections, and the first (very weak) d reflections appear approximately at the stage when the e reflections give way to b reflections. The c and d reflections remain elongate and diffuse even when the b reflections are sharp.

These observations vary somewhat from the electron

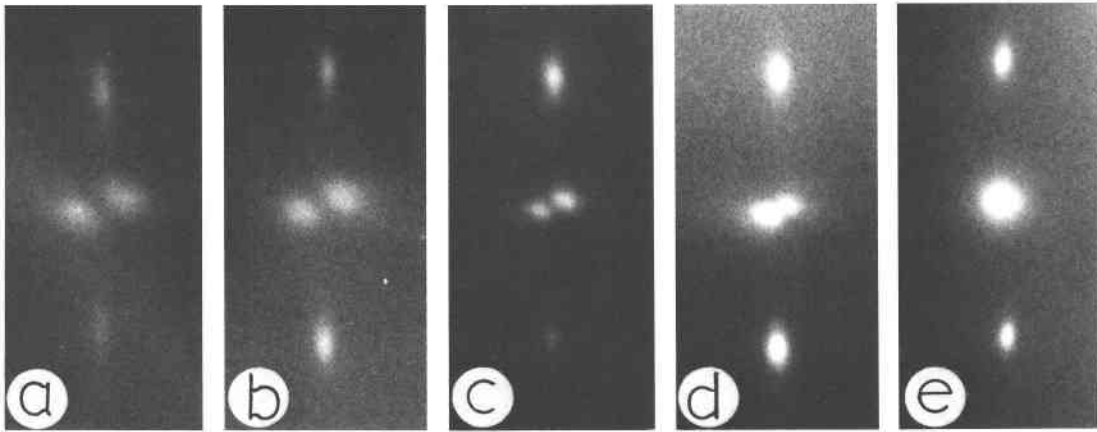


Fig. 3. Representative selection of portions of diffraction patterns showing e and b reflections (central) and elongate c reflections (top and bottom). The most disordered state in this sequence is represented by diffraction pattern (a) with highly diffuse e reflections, and the most ordered state by diffraction pattern (e) with a relatively sharp b reflection. The e reflections become progressively sharper, as well as rotating and becoming closer together, with increasing Al-Si order.

diffraction results presented by John and Müller (1988) for synthetic anorthite crystals produced under similar conditions. John and Müller reported the presence of diffuse b reflections but apparently did not observe diffuse e reflections. It is possible that the latter were overlooked, however, because the appropriate nonstandard reciprocal lattice sections were not recorded. For example, e reflec-

tions in highly disordered crystals are some distance out of the b^* - c^* plane of the reciprocal lattice, and a diffraction pattern in this orientation would therefore show only a reflections and diffuse c reflections, as observed by John and Müller. In orientations closer to the plane of the e reflections, the diffuse intensity could appear to be at and around the b positions.

The transition with annealing time of the IC structure with e reflections to the commensurate structure with b reflections appears to be continuous within the resolution of the present experiments. Two samples (ANC72, 47 min at 1400 °C; ANC73, 192 h at 1200 °C) were prepared in an attempt to pinpoint the changeover more precisely. When the e reflections become very close together, however, it is not easy to distinguish pairs of reflections that are truly discrete from single elongate b reflections. The interpretation and measurement of $|2s|^{-1}$ is thus much less reliable in this interval. Furthermore, some regions of anorthite in these two samples appeared to give b reflections, whereas others apparently gave e reflections, suggesting some variation in the degree of order within individual cubes of product material. To prepare a time-temperature-transition (TTT) diagram for the transition, the boundary between IC and $I\bar{1}$ fields has been placed immediately after samples which give at least one diffraction pattern containing suspected e reflections. (The apparently out-of-sequence presence of diffuse reflections in two diffraction patterns from ANC45 has been excluded from this analysis.) On an Arrhenius form of TTT diagram (Fig. 6), the transition can then be represented by a straight line giving an activation energy, ΔH^* , of 135 ± 14 kcal/mol. This value of ΔH^* probably reflects a rate-determining step involving Al-Si exchanges between tetrahedral sites and is in the same range as the value of 123 ± 5 kcal/mol obtained by Grove et al. (1984) for the homogenization of Huttenlocher exsolution lamellae in natural crystals of anorthite-rich plagioclase.

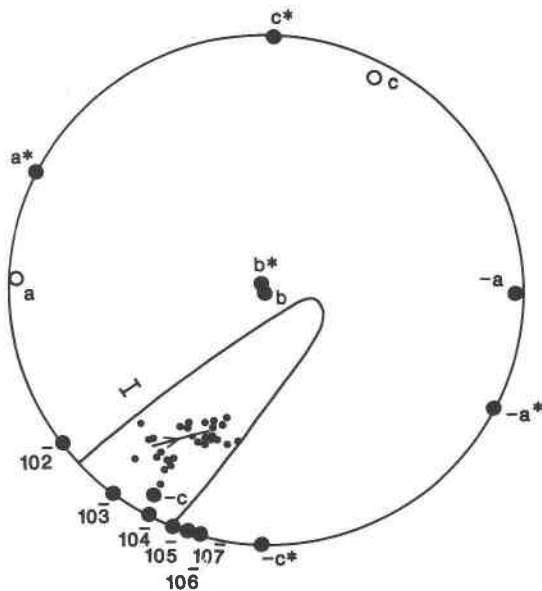


Fig. 4. Stereographic projection to represent the orientation of the IC vector s in synthetic anorthites. Each point represents the best estimate for a single sample, and an arrow indicates the direction of change of orientation of s with annealing time. The error bar indicates an uncertainty of $\sim \pm 5^\circ$. The approximate limits of the orientations of s in natural intermediate plagioclases are indicated by a continuous line (after Grove, 1977; Smith and Brown, 1988).

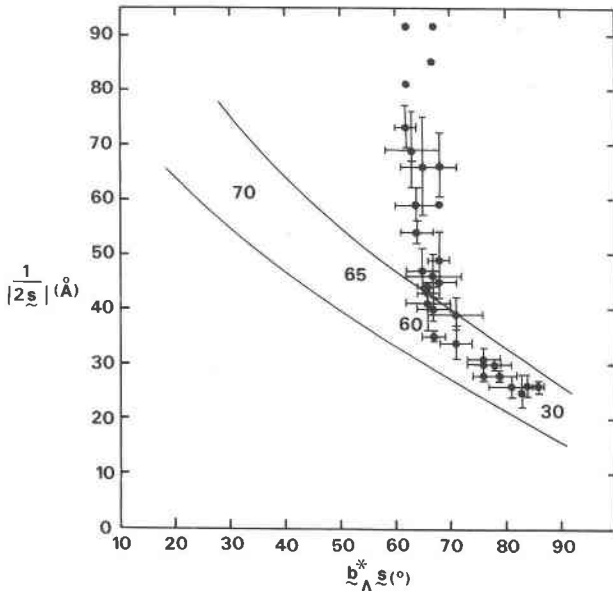


Fig. 5. Variation of spacing, $1/|2s|$, with orientation, $b^* \Delta s$, for the IC structure as measured from electron diffraction patterns for synthetic anorthites. Continuous lines represent the approximate limits of the equivalent variation in natural intermediate plagioclases for compositions indicated in mole percent anorthite component. The anorthite and intermediate plagioclase data are indistinguishable for compositional equivalents of $\sim An_{30} \sim An_{55}$. (Data given in full in Table 1 of Carpenter, 1991b.)

The size, δ , of type b APDs that develop once the synthetic anorthite crystals have achieved $I\bar{1}$ order appears to be related to the repeat distance of the last e modulations. This is seen most conveniently in a plot of $|2s|$ and $1/\delta$ against the logarithm of annealing time, t (Fig. 7). The earliest crystals have relatively small real space distances for the incommensurate repeat and the ordering process is characterized by a steady increase in this length. Growth of type b APDs takes over as the domain coarsening mechanism when the spacing between periodic APBs of the IC structure ($|2s|^{-1}$) exceeds $\sim 90 \text{ \AA}$, the coarsest repeat observed. In the absence of dark field images of the APB distribution in the IC structure, it is possible only to speculate that the APBs of the $I\bar{1}$ crystals are inherited from the IC structure by the loss of a preferred orientation. Wenk and Nakajima (1979, 1980) and Wenk et al. (1980) have discussed how such a transition might occur from a microstructural point of view, but they were considering natural plagioclase feldspars with compositions close to $\sim An_{65}$.

At 1100, 1200, and 1400 °C, the variation of $|2s|$ with $\ln t$ is approximately linear. No theoretical justification for this can be offered at present, but as shown in Carpenter (1991b), the square of the macroscopic order parameter also varies approximately linearly with $\ln t$. The degree of Al-Si order evidently controls the repeat distance of the IC structure. Variations of $|2s|$ in samples annealed at $\sim 1300 \text{ }^\circ\text{C}$ are not so clear cut (Fig. 7) since

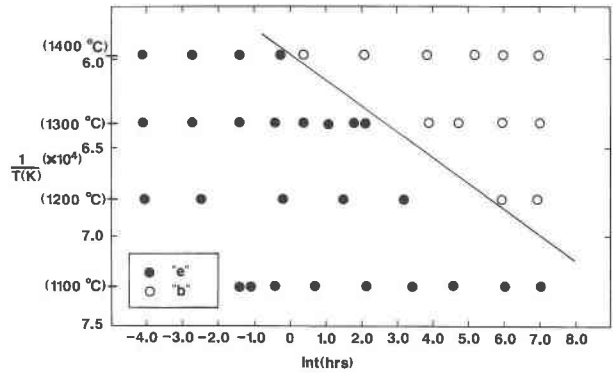


Fig. 6. Arrhenius form of a TTT diagram, showing the transition from crystals with e reflections to crystals with b reflections. The straight line drawn in by eye gives an activation energy of 135 kcal/mol with an uncertainty of ± 14 kcal/mol.

there is considerable scatter between samples given approximately the same heat treatment. Two of the samples (ANC46 and ANC17) show a split population of values of $|2s|$ and $b^* \Delta s$, and one sample that was predominantly ordered with sharp b reflections (ANC45) quite unexpectedly and out of sequence also gave two diffraction patterns with diffuse e reflections. A possible explanation for this heterogeneity relates to the degree of order that is incorporated into the crystals as they nucleate and grow. Crystallization almost certainly occurs while the cubes of glass are being heated from room temperature to the furnace temperature and may not occur uniformly in the core and rim zones. Either a greater range of crystals, in terms of their positions within the cubes, have by chance been examined in the 1300 °C samples, or crystallization at this temperature is especially sensitive to the time-temperature pathway followed by the glass.

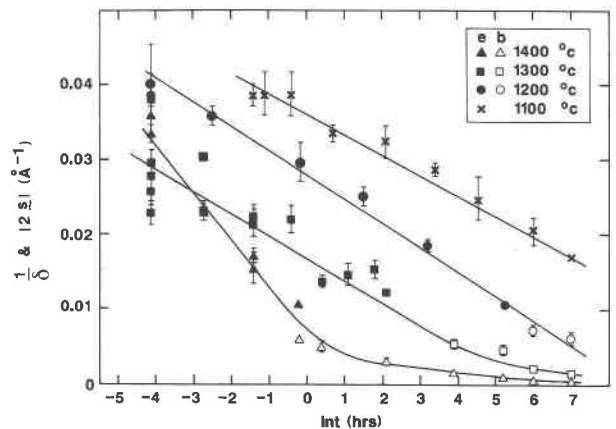


Fig. 7. Variation of $1/\delta$ and $|2s|$ with the natural logarithm of annealing time (t), where δ is the mean size of type b domains. The transition between structures with e and b domains could be continuous, though the data for 1300 °C annealing experiments show a considerable scatter.

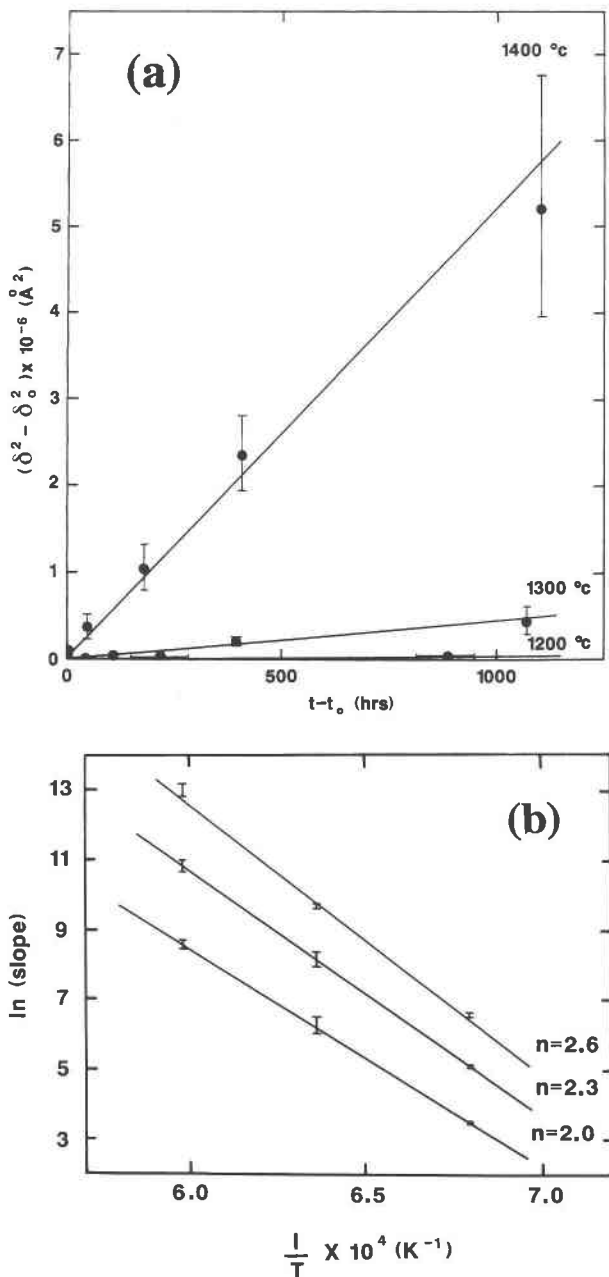


Fig. 8. Kinetic data for coarsening of type b APDs. (a) The domain size variations are consistent with $(\delta^2 - \delta_0^2)$ proportional to annealing time, $t - t_0$. The APD size at time t is represented by δ and δ_0 is the "initial" domain size at time t_0 . Equivalent plots of $(\delta^{2.3} - \delta_0^{2.3})$ and $(\delta^{2.6} - \delta_0^{2.6})$ against $t - t_0$ also give straight line relationships. (b) Arrhenius plots of the logarithm of the slopes from a as a function of $1/T$ for three different values of n . At $n = 2.6$ the three data points no longer lie on a straight line.

APD COARSENING

Isothermal APD coarsening is expected to follow a well-established rate law of the form

$$\delta^n - \delta_0^n = nk e^{(-\Delta H^*/RT)} (t - t_0) \quad (1)$$

where δ is the average domain diameter, δ_0 is the initial domain diameter at time t_0 , ΔH^* is an activation energy, R is the gas constant, and $t - t_0$ is the annealing time. For APD coarsening in metals, a value of $n = 2$ is typically found (English, 1966; Poquette and Mikkola, 1969; Sakai and Mikkola, 1971; Sauthoff, 1973; Ardell et al., 1979; Allen and Cahn, 1979), whereas observed values of $n > 2$ are usually rationalized in terms of the dragging effects of impurity atoms adsorbed on the APBs (Ling and Starke, 1971; Rase and Mikkola, 1975; Bley and Fayard, 1976; Morris et al., 1976; Allen and Krzanowski, 1982). Among oxide and silicate systems, Nord and Lawson (1988) found $n = 2.44$ for twin domain coarsening in crystals of composition $\text{Ilm}_{70}\text{Hem}_{30}$ in the ilmenite-hematite solid solution series, Carpenter (1979) measured $n \approx 10$ for APD coarsening in pigeonite, and Carpenter (1981) suggested a value of $n \approx 8$ to explain APD sizes in natural omphacite.

In testing the coarsening law for APDs in anorthite using the data given in Table 1, it was necessary to choose values of δ_0 and t_0 to allow for the early stages of IC ordering. A value of $\delta_0 = 90 \text{\AA}$ was selected since it is the largest value of $|2s|^{-1}$ observed. Values of t_0 were then estimated for each temperature from the curves shown in Figure 6 as the time at which $|2s| = 1/90 \text{\AA}^{-1}$ was reached. This gives $t_0 = 181 \text{ h}$ at $1200 \text{ }^\circ\text{C}$, 6.7 h at $1300 \text{ }^\circ\text{C}$, and 0.5 h at $1400 \text{ }^\circ\text{C}$. Alternative values of δ_0 and t_0 do not have a critical influence on the following analysis.

Figure 8a shows that, within experimental error, $(\delta^2 - \delta_0^2)$ is linear with $t - t_0$. Larger values of n cannot be excluded, however, and the upper limit for n that is still compatible with the observed coarsening is ~ 2.6 . Müller et al. (1984) suggested $n = 2.75$ for APD coarsening in anorthite at $1430 \text{ }^\circ\text{C}$, but they had fewer observations to consider. Arrhenius plots of the slopes from $(\delta^n - \delta_0^n)$ against t yield activation energies of $123 \pm 2 \text{ kcal/mol}$ for $n = 2$, $139 \pm 5 \text{ kcal/mol}$ for $n = 2.3$, and $\sim 152 \text{ kcal/mol}$ for $n = 2.6$ (Fig. 8b). The results for $n = 2.6$ do not give a strictly linear Arrhenius relationship, confirming this as being an upper boundary for the value of n . Values of n in the lower range are also more likely, given that the activation energy for the "e" $\rightarrow I\bar{1}$ transition is $135 \pm 14 \text{ kcal/mol}$ and that for the overall ordering rate it is $124 \pm \sim 15 \text{ kcal/mol}$ (Carpenter, 1991b). In Equation 1, the coefficient k has units of length squared per unit time if $n = 2$; values of $0.44 \times 10^{-4} - 2.40 \times 10^{-4} \text{\AA}^2/\text{h}$ ($= 1.22 - 6.67 \times 10^{-24} \text{ cm}^2/\text{s}$), $0.021 - 0.342 \text{\AA}^{2.3}/\text{h}$ and $\sim 32.6 \text{\AA}^{2.6}/\text{h}$ are obtained from the intercepts (at $1/T = 0$) in Figure 8b for $n = 2, 2.3$, and 2.6 , respectively.

On an atomic scale, APD coarsening is achieved by exchange of Al and Si between tetrahedral sites at the APBs. The measured activation energy presumably indicates the energy barrier for this process and is comparable with the activation energy for $\text{Na} + \text{Si} \rightleftharpoons \text{Ca} + \text{Al}$ interdiffusion in Ca-rich plagioclase (Grove et al., 1984). A physical explanation of the phenomenological parameter k is not so readily apparent. Allen and Cahn (1979) proposed that k depends on a geometrical coefficient re-

lating the square of the mean curvature of the APBs to the square of their surface area, the gradient energy for the order parameter, Q , and a kinetic coefficient relating $\partial Q/\partial t$ to $\partial G/\partial Q$. They concluded that, for second or higher order transitions, k does not depend explicitly on the energy of the APBs. On the other hand, Ardell et al. (1979) developed a model in which k varies with the APB surface energy and the inverse of the order parameter, along with some other parameters. In the case of anorthite, some suggestion of how the energy of the APBs varies with temperature is provided by calorimetric data (Carpenter, 1991b), and at 1200 °C the APB energy per unit area may be a factor of approximately 2 less than at 1400 °C. If this energy did appear explicitly in the k term, it would cause the coarsening at 1200 °C to be slower, relative to the rate at 1400 °C, than would be predicted by a purely Arrhenius temperature dependence. The data do not provide sufficient constraints on the coefficients to distinguish between these models, but if the surface energy is important, the real activation energy might be ~ 10 –15% less than the apparent values obtained from Figure 8b.

Close adherence to a parabolic rate law would be consistent with ideal behavior of the APBs in anorthite, that is, with no impurity drag effects. A definitive determination of the precise value of n must await further experiments, however, preferably using starting crystals of anorthite prepared with some constant domain size.

DISCUSSION

The IC structure that develops under nonequilibrium conditions in anorthite has a well-defined orientation and repeat distance that can be followed as a function of annealing time and temperature. Its close resemblance to the ordered superstructure of intermediate plagioclase feldspars sheds new light on some of the issues still outstanding with regard to the stability and structural evolution of the natural samples. There is now general agreement that IC structures owe their stability to interactions between at least two ordering processes (see reviews by Bruce and Cowley, 1981; Heine and McConnell, 1984; McConnell, 1988). In this context, models of the IC structure of plagioclases characteristically involve interactions between albite-like and anorthite-like slabs or some combination of Al-Si ordering with Na-Ca ordering (see recent reviews by Horst, 1984; Kitamura and Morimoto, 1984; McConnell, 1988; Smith and Brown, 1988). One of the difficulties in developing such models has been that, in addition to analyzing the expected ordering processes, it has been necessary to consider the possibility of compositional modulations. The IC structure has even been compared with structures arising from spinodal unmixing (e.g., Morimoto, 1979; Fleet, 1981). The existence of closely analogous superstructures in pure $\text{CaAl}_2\text{Si}_2\text{O}_8$ strongly suggests that the compositional variable can only be of secondary importance in determining the ordering patterns, however, and the primary problem may be reduced to one of pure order-disorder.

The first question to address concerns the nature of the

two interacting ordering processes that occur in pure anorthite. Because of the low symmetry of the system and the known behavior of many end-member feldspar phases, the choice of possible order parameters seems to be restricted to three. One component must be $Q_{\text{od}}^{\text{II}}$ for the $C\bar{1} = I\bar{1}$ Al-Si ordering transition, but the second could be either Q for the $C2/m = C\bar{1}$ displacive transition or $Q_{\text{od}}^{\text{CI}}$ for the $C2/m = C\bar{1}$ Al-Si ordering transition. The coupling mechanism is likely to be a result of the common strain such that a change in one order parameter causes a lattice distortion that then influences the second order parameter and vice versa (Salje, 1985, 1987a, 1987b; Salje et al., 1985; Salje and Devarajan, 1986; Putnis et al., 1987; Carpenter, 1988; Carpenter, 1991a). The likelihood of coupling between Q , $Q_{\text{od}}^{\text{CI}}$, and $Q_{\text{od}}^{\text{II}}$ and its possible strength may be assessed qualitatively by inspection of the spontaneous strain components associated with each order parameter. Salje et al. (1985) showed that in albite

$$Q \propto \sim x_4 \approx -\cos \alpha^* \quad (2)$$

and

$$Q_{\text{od}}^{\text{CI}} \propto \sim x_6 \approx \cos \gamma \quad (3)$$

where x_4 and x_6 are components of the spontaneous strain tensor for the $C2/m = C\bar{1}$ transition and α^* and γ are lattice parameters. In this case, x_1 , x_2 , x_3 , and x_5 are identically zero. All six components of the strain tensor for the $C\bar{1} = I\bar{1}$ transition can be nonzero, although it is found experimentally that the strain accompanying $Q_{\text{od}}^{\text{II}}$ has x_1 – x_5 small relative to x_6 (Carpenter, 1991b). Distortions accompanying the displacive $C2/m = C\bar{1}$ transition in anorthite should not be fundamentally different from those accompanying the same transition in albite, and intuitively, therefore, coupling between $Q_{\text{od}}^{\text{CI}}$ and $Q_{\text{od}}^{\text{II}}$ via x_6 might be anticipated. The relative unimportance of x_4 and hence of Q is borne out by the insensitivity of $\cos \alpha^*$ to order-disorder changes in both anorthite itself and in the intermediate plagioclases (see Fig. 12b of Carpenter, 1988, for example). Furthermore, x_6 is positive ($\gamma > 90^\circ$) for $C\bar{1}$ ordering and negative ($\gamma < 90^\circ$) for $I\bar{1}$ ordering so that $C\bar{1}$ and $I\bar{1}$ schemes are likely to coexist only in an IC configuration. A qualitative description of the IC ordering in anorthite could therefore involve modulations in $Q_{\text{od}}^{\text{CI}}$ and $Q_{\text{od}}^{\text{II}}$ with energetically favorable coupling terms. This is, of course, close to the albite-like-anorthite-like slab models except that only the degree and symmetry of the Al-Si ordering varies with distance through the crystal.

The next question concerns the possible evolution of the IC structures with temperature, pressure, and composition. In anorthite, the vector \mathbf{s} changes continuously with increasing Al-Si order and the trend is toward the $I\bar{1}$ structure, i.e., increasing $Q_{\text{od}}^{\text{II}}$. The same trend is well known in the intermediate plagioclases; $|\mathbf{2s}|^{-1}$ increases in natural ordered samples as the stability field of the $I\bar{1}$ structure is approached by adding $\text{CaAl}_2\text{Si}_2\text{O}_8$ in solid solution. If the magnitude of $Q_{\text{od}}^{\text{II}}$ really is the dominant

factor, then it seems likely that at a fixed composition, of $\sim An_{65}$ say, the real space repeat distance of the IC structure should increase during cooling, in line with normal expectations of increasing equilibrium order with falling temperature. Volume changes associated with any type of ordering in calcic plagioclases are relatively small (Carpenter et al., 1985; Carpenter, 1991b), and it is unlikely that pressure would have much direct influence on the stability of the possible ordered structures.

From Figure 5 it is clear that the orientation and magnitude of the IC vector s are interdependent. The same is also true for the intermediate plagioclase structure, and many suggestions have been made as to how this interdependence may be rationalized. The overlap in Figure 5 between natural feldspars and synthetic anorthite again suggests that composition need not be the main factor. Fleet (1981, 1982, 1984) has shown that the orientational behavior can be addressed from a macroscopic point of view by taking alternating albite-rich and anorthite-rich slabs and finding the interface between them that has the lowest energy. A judicious selection of lattice parameters leads to calculated orientations that are in reasonable agreement with the observed orientations. The lattice parameters are far more sensitive to structural state than to composition, however. For example, in the relatively disordered "high" plagioclase series, a , b , c , α and β vary by less than $\sim 0.5\%$ (using the data set of Carpenter et al., 1985). The value of γ changes by just over 1%, but much of this is probably due to $I\bar{1}$ ordering in the Ca-rich members. On the other hand, the total variation possible between different structural states is ~ 0.5 – 1.0% for a , b , c , α , and β and $\sim 4\%$ for γ . In other words, when selecting parameters to test lowest energy interface models, it is the structural state of the slabs and not their composition that is critical. There are no symmetry constraints on the orientation of s , and the elastic energy of the modulations must play some role in determining its dependence on Q_{od}^{CI} and $Q_{od}^{I\bar{1}}$.

It should be stressed that not all the features of ordering in intermediate plagioclase feldspars are reproduced by the metastable IC ordering in anorthite. In particular, f reflections have not been observed in the synthetic samples, and there is a marked divergence between the $|2s|^{-1}$ against $b^* \wedge s$ relationships at a composition equivalent of $\sim An_{55}$ (Fig. 5). No satisfactory explanation of these differences can be put forward here, but it is tempting to speculate on another aspect of the observed behavior. The "e" $\rightarrow I\bar{1}$ transition with time in anorthite appears to be continuous, with the APBs of the IC structure developing into APBs of the $I\bar{1}$ structure by the loss of their preferred orientation. Might a continuous pathway be available also for the equilibrium transition "e" $\rightleftharpoons I\bar{1}$ suggested for some intermediate compositions by Carpenter (1986)? More evidence is required, but the question has important implications for the form of the plagioclase phase diagram.

Kinetic aspects of the ordering in anorthite are probably less controversial. First, it is evident that the IC struc-

ture can be kinetically favored when ordering occurs under nonequilibrium conditions in the equilibrium stability field of the $I\bar{1}$ structure. This applies both to anorthite (this paper) and to some intermediate plagioclase feldspars (Carpenter, 1986). An activation energy of ~ 120 – 150 kcal/mol appears to be characteristic of the ordering reaction, APD coarsening, and $Na + Si = Ca + Al$ interdiffusion in calcic plagioclases under dry conditions at 1 atm pressure. The rate-determining step presumably involves breaking of Al-O or Si-O bonds. As discussed at greater length in Carpenter (1991b), correlations between the local exchanges over a longer range to give incommensurate or commensurate ordering are probably influenced by the bending of semiflexible Al,Si-O-Al,Si linkages.

ACKNOWLEDGMENTS

I wish particularly to thank R. Morrell of the National Physical Laboratory for preparing the anorthite glass and E. Salje for his continuing guidance concerning order parameter behavior. R.J. Angel, T.L. Grove, and G.L. Nord, Jr., are thanked for their critical reviews of the manuscript, which led to a number of improvements. The work was supported by a grant from the Natural Environment Research Council of Great Britain (GR3/5547) and a Science Research Fellowship from the Nuffield Foundation, both of which are gratefully acknowledged. This paper is Cambridge Earth Sciences contribution no. 1811.

REFERENCES CITED

- Allen, S.M., and Cahn, J.W. (1979) A microscopic theory for antiphase boundary motion and its application to antiphase domain coarsening. *Acta Metallurgica*, 27, 1085–1095.
- Allen, S.M., and Krzanowski, J.E. (1982) Fundamental studies of the migration kinetics of coherent interfaces in ordered alloys. In H.I. Aaronson, D.E. Laughlin, R.F. Sekerka, and C.M. Wayman, Eds., *Proceedings of an international conference on solid \rightarrow solid phase transformations*, p. 225–229. The Metallurgical Society of AIME, Warrendale, Pennsylvania.
- Ardell, A.J., Mardesich, N., and Wagner, C.N.J. (1979) Antiphase domain growth in Cu₃Au: Quantitative comparison between theory and experiment. *Acta Metallurgica*, 27, 1261–1269.
- Benna, P., Zanini, G., and Bruno, E. (1985) Cell parameters of thermally treated anorthite. Al/Si configurations in the average structures of the high temperature calcic plagioclases. *Contributions to Mineralogy and Petrology*, 90, 381–385.
- Bley, F., and Fayard, M. (1976) Cinétique de grossissement des domaines ordonnés dans des alliages Ni₃Fe_{1-x}Al_x. *Acta Metallurgica*, 24, 575–580.
- Brown, W.L. (1984) Feldspars and feldspathoids: Structures, properties and occurrences. NATO ASI series C, 137, 541 p. Reidel, Dordrecht.
- Bruce, A.D., and Cowley, R.A. (1981) *Structural phase transitions*, 326 p. Taylor and Francis, London.
- Carpenter, M.A. (1979) Experimental coarsening of antiphase domains in a silicate mineral. *Science*, 206, 681–683.
- (1981) Omphacite microstructures as time-temperature indicators of blueschist- and eclogite-facies metamorphism. *Contributions to Mineralogy and Petrology*, 78, 441–451.
- (1986) Experimental delineation of the "e" $\rightleftharpoons I\bar{1}$ and "e" $\rightleftharpoons C\bar{1}$ transformations in intermediate plagioclase feldspars. *Physics and Chemistry of Minerals*, 13, 119–139.
- (1988) Thermochemistry of aluminum/silicon ordering in feldspar minerals. In E.K.H. Salje, Ed., *Physical properties and thermodynamic behaviour of minerals*. NATO ASI series C, 225, p. 265–323. Reidel, Dordrecht.
- (1991a) Thermodynamics of phase transitions in minerals: A macroscopic approach. In N.L. Ross and G.D. Price, Eds., *Stability of minerals*. Unwin Hayman, London.
- (1991b) Mechanisms and kinetics of Al-Si ordering in anorthite:

- II. Energetics and a Ginzburg-Landau rate law. *American Mineralogist*, 76, 1120–1133.
- Carpenter, M.A., and Salje, E. (1989) Time-dependent Landau theory for order/disorder processes in minerals. *Mineralogical Magazine*, 53, 483–504.
- Carpenter, M.A., McConnell, J.D.C., and Navrotsky, A. (1985) Enthalpies of ordering in the plagioclase feldspar solid solution. *Geochimica et Cosmochimica Acta*, 49, 947–966.
- Carpenter, M.A., Angel, R.J., and Finger, L.W. (1990) Calibration of Al/Si order variations in anorthite. *Contributions to Mineralogy and Petrology*, 104, 471–480.
- Davis, G.L., and Tuttle, O.F. (1952) Two new crystalline phases of the anorthite composition, $\text{CaO} \cdot \text{Al}_2\text{O}_3 \cdot 2\text{SiO}_2$. *American Journal of Science*, Bowen Volume, 107–114.
- Effenberger, H. (1980) Petalite, $\text{LiAlSi}_4\text{O}_{10}$: Verfeinerung der Kristallstruktur, Diskussion der Raumgruppe und Infrarot-Messung. *Tschermaks Mineralogische und Petrographische Mitteilungen*, 27, 129–142.
- English, A.T. (1966) Long-range ordering and domain-coalescence kinetics in Fe-Co-2V. *Transactions of the Metallurgical Society of AIME*, 236, 14–18.
- Fleet, M.E. (1981) The intermediate plagioclase structure: An explanation from interface theory. *Physics and Chemistry of Minerals*, 7, 64–70.
- (1982) Orientation of compositional modulation in plagioclase feldspar. In H.I. Aaronson, D.E. Laughlin, R.F. Sekerka, and C.M. Wayman, Eds., *Proceedings of an international conference on solid → solid phase transformations*, p. 197–201. The Metallurgical Society of AIME, Warrendale, Pennsylvania.
- (1984) Orientation of feldspar intergrowths: Application of lattice misfit theory to cryptoperthites and e-plagioclase. *Bulletin de Minéralogie*, 107, 509–519.
- Goldsmith, J.R., and Laves, F. (1956) Crystallization of metastable disordered anorthite at “low temperatures.” *Zeitschrift für Kristallographie*, 107, 396–405.
- Grove, T.L. (1977) A periodic antiphase structure model for the intermediate plagioclases (An_{33} to An_{73}). *American Mineralogist*, 62, 932–941.
- Grove, T.L., Baker, M.B., and Kinzler, R.J. (1984) Coupled CaAl-NaSi diffusion in plagioclase feldspar: Experiments and applications to cooling rate speedometry. *Geochimica et Cosmochimica Acta*, 48, 2113–2121.
- Heine, V., and McConnell, J.D.C. (1984) The origin of incommensurate structures in insulators. *Journal of Physics C*, 17, 1199–1220.
- Horst, W. (1984) Modulated structures in intermediate plagioclases—history, ideas and perspectives. *Fortschritte der Mineralogie*, 62, 107–154.
- John, R.-J., and Müller, W.F. (1988) Experimental studies on the kinetics of order-disorder processes in anorthite, $\text{CaAl}_2\text{Si}_2\text{O}_8$. *Neues Jahrbuch für Mineralogie Abhandlungen*, 3, 283–295.
- Kitamura, M., and Morimoto, N. (1984) The modulated structure of the intermediate plagioclase and its change with composition. In W.L. Brown, Ed., *Feldspars and feldspathoids: Structures, properties and occurrences*. NATO ASI Series C, 137, p. 95–119. Reidel, Dordrecht.
- Klein, L., and Uhlmann, D.R. (1974) Crystallization behaviour of anorthite. *Journal of Geophysical Research*, 79, 4869–4874.
- Kroll, H., and Müller, W.F. (1980) X-ray and electron-optical investigation of synthetic high-temperature plagioclases. *Physics and Chemistry of Minerals*, 5, 255–277.
- Ling, Fu-Wen, and Starke, E.A., Jr. (1971) The development of long-range order and the resulting strengthening effects in Ni_3Mo . *Acta Metallurgica*, 19, 759–768.
- McConnell, J.D.C. (1988) The thermodynamics of short range order. In E.K.H. Salje, Ed., *Physical properties and thermodynamic behaviour of minerals*. NATO ASI series C, 225, p. 17–48. Reidel, Dordrecht.
- McLaren, A.C. (1974) Transmission electron microscopy of the feldspars. In W.S. MacKenzie and J. Zussman, Eds., *The feldspars*, p. 378–423. Manchester University Press, Manchester, England.
- Morimoto, N. (1979) The modulated structures of feldspars. In J.M. Cowley, J.B. Cohen, M.B. Salamon, and B.J. Wuensch, Eds., *Modulated structures—1979*. Proceedings of the American Institute of Physics, 53, 299–310.
- Morris, D.G., Brown, G.T., Piller, R.C., and Smallman, R.E. (1976) Ordering and domain growth in Ni_3Fe . *Acta Metallurgica*, 24, 21–28.
- Müller, W.F., John R.J., and Kroll, H. (1984) On the origin and growth of antiphase domains in anorthite. *Bulletin de Minéralogie*, 107, 489–494.
- Nord, G.L., Jr., and Lawson, C.A. (1988) Order-disorder transition in $\text{Fe}_2\text{O}_3\text{-FeTiO}_3$: Structure and migration kinetics of transformation-induced twin domain boundaries. In G.W. Lorimer, Ed., *Phase transformations*, 87, p. 578–580. Institute of Metals, London.
- Poquette, G.E., and Mikkola, D.E. (1969) Antiphase domain growth in Cu_3Au . *Transactions of the Metallurgical Society of AIME*, 245, 743–751.
- Putnis, A., Salje, E., Redfern, S.A.T., Fyfe, C.A., and Strobl, H. (1987) Structural states of Mg-cordierite I: Order parameters from synchrotron X-ray and NMR data. *Physics and Chemistry of Minerals*, 14, 446–454.
- Rase, C.L., and Mikkola, D.E. (1975) Effect of excess Au on antiphase domain growth in Cu_3Au . *Metallurgical Transactions*, 6A, 2267–2271.
- Sakai, M., and Mikkola, D.E. (1971) The growth of antiphase domains in Cu_3Au as studied by transmission electron microscopy. *Metallurgical Transactions*, 2, 1635–1641.
- Salje, E. (1985) Thermodynamics of sodium feldspar I: Order parameter treatment and strain induced coupling effects. *Physics and Chemistry of Minerals*, 12, 93–98.
- (1987a) Thermodynamics of plagioclases I: Theory of the $\bar{1}\bar{1}$ -P1 transition in anorthite and Ca-rich plagioclases. *Physics and Chemistry of Minerals*, 14, 181–188.
- (1987b) Structural states of Mg-cordierite II: Landau theory. *Physics and Chemistry of Minerals*, 14, 455–460.
- (1988a) Structural phase transitions and specific heat anomalies. In E.K.H. Salje, Ed., *Physical properties and thermodynamic behaviour of minerals*. NATO ASI series C, 225, p. 75–118. Reidel, Dordrecht.
- (1988b) Toward a thermodynamic understanding of feldspars: Order parameters of Na-feldspar and the $\bar{1}\bar{1}$ -P1 phase transition in anorthite. In S. Ghose, J.M.D. Coey, and E. Salje, Eds., *Structural and magnetic phase transitions in minerals*. Advances in Physical Geochemistry, 7, p. 1–16. Springer-Verlag, New York.
- (1989) Towards a better understanding of time-dependent geological processes: Kinetics of structural transformations in minerals. *Terra Nova*, 1, 35–44.
- Salje, E., and Devarajan, V. (1986) Phase transitions in systems with strain-induced coupling between two order parameters. *Phase Transitions*, 6, 235–248.
- Salje, E., Kuscholke, B., Wruck, B., and Kroll, H. (1985) Thermodynamics of sodium feldspar II: Experimental results and numerical calculations. *Physics and Chemistry of Minerals*, 12, 99–107.
- Sauthoff, G. (1973) Growth kinetics and size distribution of ordered domains in Cu_3Au . *Acta Metallurgica*, 21, 273–279.
- Schreyer, W., and Schairer, J.F. (1962) Metastable osumilite- and petalite-type phases in the system $\text{MgO-Al}_2\text{O}_3\text{-SiO}_2$. *American Mineralogist*, 47, 90–104.
- Smith, J.V., and Brown, W.L. (1988) *Feldspar minerals. 1: Crystal structures, physical, chemical and microtextural properties* (2nd edition), 828 p. Springer-Verlag, New York.
- Takéuchi, Y., and Donnay, G. (1959) The crystal structure of hexagonal $\text{CaAl}_2\text{Si}_2\text{O}_8$. *Acta Crystallographica*, 12, 465–470.
- Takéuchi, Y., Haga, N., and Ito, J. (1973) The crystal structure of monoclinic $\text{CaAl}_2\text{Si}_2\text{O}_8$: A case of monoclinic structure closely simulating orthorhombic symmetry. *Zeitschrift für Kristallographie*, 137, 380–398.
- Wenk, H.-R., and Nakajima, Y. (1979) Periodic superstructures in calcic plagioclases. In J.M. Cowley, J.B. Cohen, M.B. Salamon, and B.J. Wuensch, Eds., *Modulated structures—1979*. Proceedings of the American Institute of Physics, 53, 317–320.
- (1980) Structure, formation, and decomposition of APB's in calcic plagioclases. *Physics and Chemistry of Minerals*, 6, 169–186.
- Wenk, H.-R., Joswig, W., Tagai, T., Korekawa, M., and Smith, B.K. (1980) The average structure of An 62–66 labradorite. *American Mineralogist*, 65, 81–95.